Solar stimulated inelastic light scattering in clear sea water

Chuanmin Hu, Kenneth J. Voss

Department of Physics, University of Miami
Coral Gables, Fl 33124

ABSTRACT

Solar Fraunhofer lines are used as indicators of the inelastic light scattering in the sea water. Data from both in-shore and off-shore are presented and compared with results of theoretical modeling. Very good agreement is found between the modeled and measured proportion of inelastic to elastically scattered and direct light at 589nm when the Raman scattering coefficient of Marshall and Smith[1] (1990) (0.00026m^{-1}) is used, as opposed to that of Slusher and Derr[2] (1975) (0.00078m^{-1}). At 656nm the agreement is not as good, indicating possible interference from other sources such as Chlorophyll fluorescence. Recent work has extended the measurements to include smaller absorption lines, such as 689nm, where significant filling has been measured at the surface due to the Chlorophyll fluorescence. This technique allows the natural fluorescence to be measured, even at the surface where there is still a significant amount of direct solar light.

Key words: Fraunhofer lines, Raman scattering, Chlorophyll fluorescence.

1. INTRODUCTION

Inelastic light scattering plays a very important role in the underwater light field distribution[1,3,4] and has an influence on the remote sensing signal in the visible[5] as well. Three main processes are involved in the underwater inelastic light scattering: Raman scattering, fluorescence of chlorophyll a and other phytoplankton pigments[6,7], and dissolved organic matter (DOM) fluorescence[7]. Among them, Raman scattering by water molecules typically has a wavenumber shift of 3347 cm-1 and a widely accepted value 2.6 x $10^{-4}m^{-1}$ for total scattering cross section with 488nm excitation, and has been simulated well using the radiative transfer model[8,9]; chlorophyll a fluorescence has long been known to contribute to the light field in the 685nm region, while DOM fluorescence is a broad band emission that varies with both the nature and the concentration of the fluorescing compounds[7].

Direct measurement of inelastic light scattering in natural waters was not found in literature until 1992, when a system with very high spectral resolution (0.008nm/CCD pixel) was built and solar Fraunhofer lines were used to separate the elastic and inelastic light[10]. The basic idea is to measure the spectral irradiance (downwelling E_d or upwelling E_u) at Fraunhofer wavelengths both at the sea surface and in-water, and find out how much the absorption line depth varies (Fig.1). Two parameters, η, which is the ratio of line peak to background, and equivalent width (w), which is the area of line peak divided by background, are used to describe the portion of inelastic light in the total light field:

$$\eta = \frac{E(\lambda_f)}{E_b(\lambda_f)} \qquad (1) \qquad\qquad w = \int_{\lambda_1}^{\lambda_2}\left[1 - \frac{E(\lambda)}{E_b(\lambda)}\right]d\lambda \qquad (2)$$

where $E(\lambda)$ is the spectral irradiance, $E_b(\lambda)$ is the background irradiance, λ_1 and λ_2 are the starting and ending points of the Fraunhofer line, λ_f is the line peak wavelength (fig. 1a). Thus, at depth z, the ratio of inelastically scattered irradiance to total irradiance, and the ratio of direct transmitted and elastically scattered irradiance to total irradiance, are derived as:

$$\frac{E_{in}(z)}{E_t(z)} = (1 - \frac{w(z)}{w_0}) \qquad (3) \qquad\qquad \frac{E_{el}}{E_t} = \frac{w(z)}{w_0} \qquad (4)$$

where $w(z)$ and w_0 are equivalent widths at depth and surface, respectively (fig. 1b).

SPIE Vol. 2963 • 0277-786X/97/$10.00

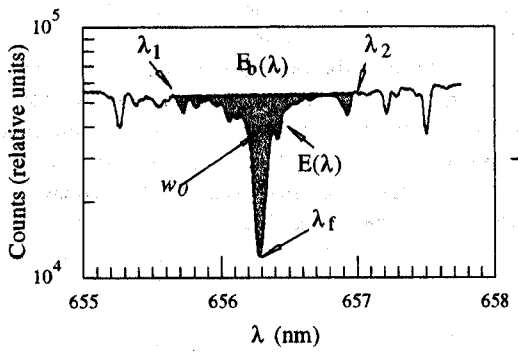

Fig. 1a. Fraunhofer line at 656nm. $E_b(\lambda)$ is the background from λ_1 to λ_2 and the peak wavelength λ_f is 656.28nm. The equivalent width (w) is the shaded area divided by the background.

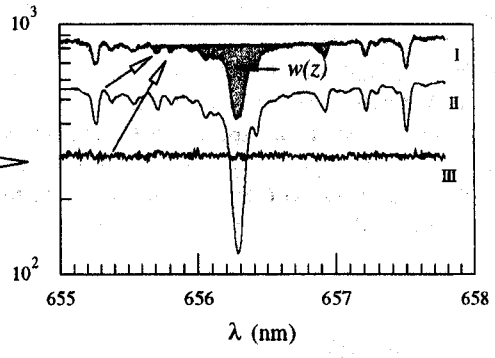

Fig. 1b. Fill-in of the Fraunhofer line. The inelastically scattered light III is added to the direct transmitted and elastically scattered light II (1% of fig. 1a), resulting in I which has a line fill-in.

Figure 1. Fraunhofer line shape at 656nm and the line filling features.

The same technique is used in this paper except that the system is rebuilt to improve its performance. Experiments show that w is a better parameter than η since w is resolution independent and does not depend only on a single point. A least square fitting procedure is used to "clean" any noisy spectra (Fig. 2). Also presented here is the data collected from both off-shore and in-shore waters. Since there is no Fraunhofer line around the 685nm region, smaller absorption lines at 689nm (Fig. 3) caused by oxygen in the atmosphere are used to detect the chlorophyll a fluorescence. This is shown to be a promising technique to measure the natural chlorophyll fluorescence.

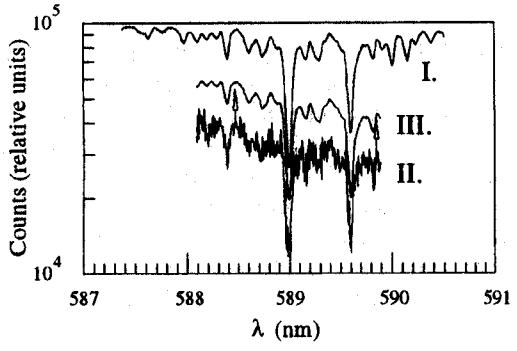

Figure 2. Fraunhofer line at 589nm. I: line at surface; II: line at depth (noisy); III: fitted from II using I as a template.

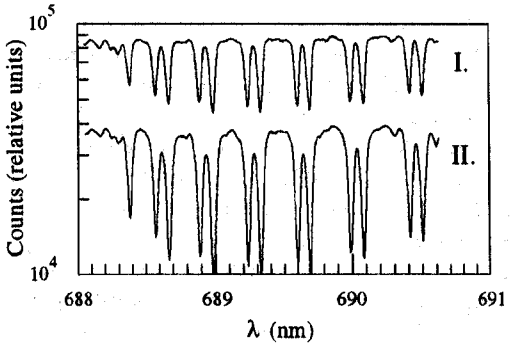

Figure 3. Oxygen absorption line at 689nm. I: measured at 1:13pm with 30s exposure time; II: measured at 6:13pm with 60s exposure time.

2. INSTRUMENTATION AND DATA ACQUISITION

The original Fraunhofer line system described elsewhere[10] has been rebuilt and improved. First, since a single, unprotected fiber is very fragile and not capable of taking measurements during harsh conditions on a cruise (in fact it was broken at least once each time it was on a cruise), a fiber bundle protected by a metal shield together with eight wire conductors is used instead (Fig. 4, part VI). We have the following components built into the instrument head (Fig. 4): two fiber optic cosine irradiance collectors (downwelling and upwelling) for the light input to the monochromator, two cosine

irradiance collectors for photocell detectors which are used to monitor the overall downwelling and upwelling irradiance level, and a depth transducer. Eight 100um core size all silica fibers are used to transmit the light from the two cosine collectors, with four in each one. Only 6 of the 8 fibers are used to measure the Fraunhofer line spectra, the remaining 2 can monitor the overall spectra for the whole visible band. However, they are not used now. A 512x512 TE cooled CCD camera is used to record the spectra. Such a configuration enables us to measure downwelling and upwelling channels simultaneously, which is a very important feature since the reference line shape at sea surface varies with time except around solar noon (Fig. 3) (An alternative way to monitor the surface reference line is to use a deck cell as a separate channel). A cross talk correction algorithm is used to separate the two spectra on the CCD.

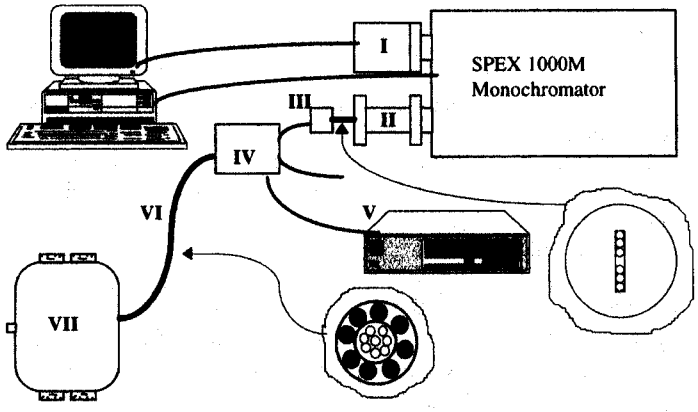

Main parts of the Fraunhofer system:
I. An OMA 4000 CCD camera;
II. Fiber adapter as F-number matcher;
III. Fiber array ferrule;
IV. Cable splicing box with 3 outputs:
1. 6 fibers as monochromator input;
2. 2 fibers to monitor the overall spectra in visible band, currently not being used;
3. Wire conductors for power supply and depth and photocell readouts;
V. Electronic control panel;
VI. 130m fiber-wire cable;
VII. Detector head which includes:
1. 2 fiber optic cosine collectors;
2. 2 photocell cosine collectors;
3. A depth transducer;
4. 2 photocell electronic boards.

Figure 4. The Fraunhofer system schematic chart.

The instrument was deployed on the research ship RV CALANUS during spring, summer and winter in the Florida Straits and Florida Bay region (Fig. 5). The whole system was aligned and adjusted to achieve its best performance. Six tracks on the CCD were chosen to record the images from the six fibers, three for downwelling and 3 for upwelling. Data were collected both in open ocean blue water and in coastal green and brownish waters where the sea bottom depth is about 6 meters. A floating frame was used to hold the instrument to collect the surface upwelling irradiance data at shallow stations. Care was taken to collect the data only when the sky was clear and the instrument was not in ship shadow. Also the measurements were taken within ± 3 hours around solar noon to make sure that the surface reference line was stable. Wind speed during the measurements was 5m/s to 10m/s and the solar zenith angle was between 15° and 25°. At some stations, pigment concentration data, one of the inputs of the simulation model, were collected by another research group.

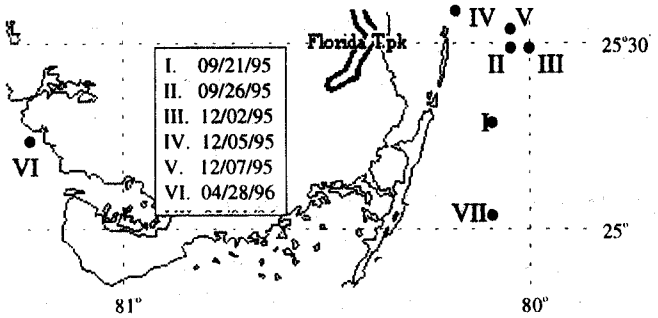

Figure 5. Locations of the data collection stations. Station IV and VI are shallow coastal green waters where the sea bottom can be seen; the other stations are clear ocean waters.

3. RESULTS AND DISCUSSION

The data were reduced by using the fitting procedure and the equivalent width calculation program. Lab experiments show that the maximum error of the algorithm for very noisy spectra is ± 5%, while another ± 5% maximum error is due to the surface reference variation. Thus, the maximum error at depth is about ± 10%. Forward Monte-Carlo simulation is used to simulate the equivalent width versus depth data[9] with a correction on the normalization of irradiance level at excitation and emission wavelengths on top of the atmosphere. When pigment concentration data is not available, it is assumed $0.1 mg/m^3$ for clear ocean water and $1 mg/m^3$ for coastal green water. DOM is not considered in the model, since the simulation results vary only a little bit even with DOM considered when DOM concentration is low, which is the case for all stations. Chlorophyll fluorescence is not considered in the simulation either. The simulation results together with the reduced data are shown in Figure 6, 7 and 8.

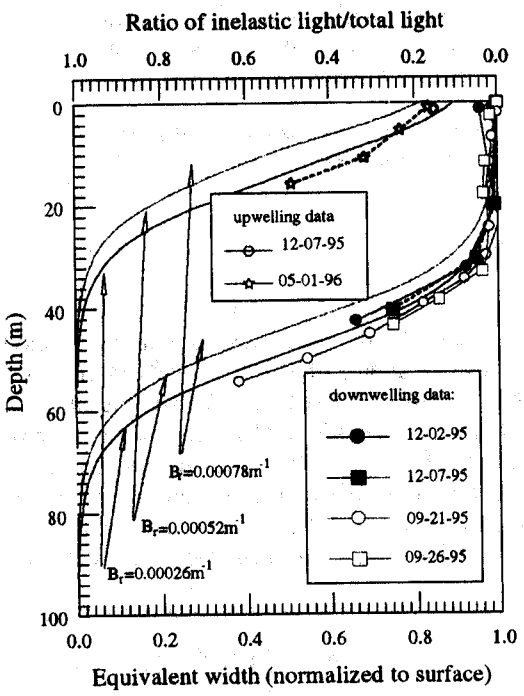

Fig. 6a. Normalized equivalent width ($w(z)/w_0$) for the Fraunhofer line at 589nm at clear water stations, both downwelling and upwelling. The simulation uses the pigment concentration, wind speed and solar zenith angle data from the 12/07/95 station. Only Raman scattering is considered in the model with the excitation wavelength at 492nm. Three different Raman scattering coefficients (B_r) are used.

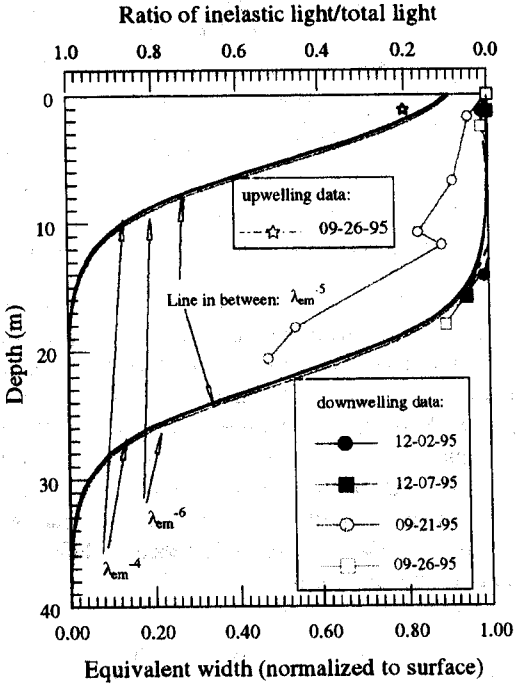

Fig. 6b. $w(z)/w_0$ as a function of depth for the Fraunhofer line at 656nm at clear water stations, both downwelling and upwelling. The simulation uses the pigment concentration, wind speed and solar zenith angle data from the 12/07/95 station. The λ_{em} dependence of the Raman scattering coefficient is assumed to be λ_{em}^{-4}, λ_{em}^{-5} and λ_{em}^{-6}, respectively.

Figure 6. Experimental data and model simulation results for Fraunhofer lines at clear water stations.

From the results in Figure 6a, it is easy to see that when the Raman scattering coefficient, $B_r=2.6\times10^{-4}m^{-1}$, from Marshall and Smith[1] is used in the simulation, the model results agree very well with the experimental ones. Also shown in the graph is that the experimental data at 589nm for clear water is very stable from station to station. Thus, $B_r=2.6\times10^{-4}m^{-1}$ for emission at 589nm is confirmed for natural water. In figure 6b, the dependence of the Raman scattering coefficient on the emission wavelength (λ_{em}) is taken to be λ_{em}^{-4}, λ_{em}^{-5} and λ_{em}^{-6}. Negligible difference is found among the results, which means this dependence is not critical in the Raman scattering simulation regardless of the discrepancy in the literature[3]. From this work, we can see that in clear ocean water, at 50m depth, half of the total downwelling irradiance at 589nm is

from Raman scattering. At 656nm this depth is about 25m. Another interesting feature in Fig. 6b is that the data is not as stable as that for 589nm. The data on 09-21-95 obviously diverge from the general trend and show us more filling, i.e., more inelastically scattered irradiance than the model predicted value. Since the model does not consider chlorophyll or DOM fluorescence, the discrepancy is probably due to one or both of these sources.

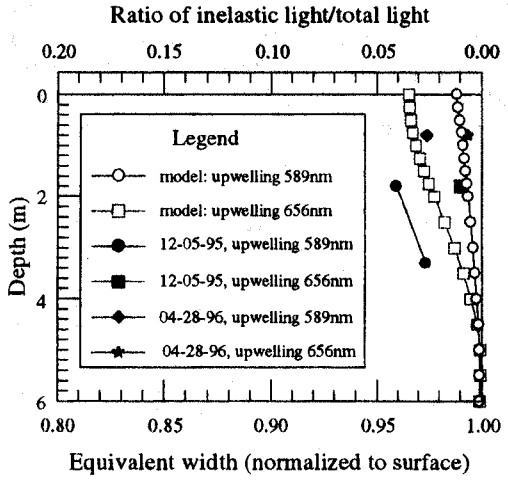

Figure 7. Monte-Carlo simulation and experimental data for coastal green water at 589nm and 656nm. In the model, pigment concentration is taken to be $1 mg/m^3$, and a 6m sea bottom with reflectance 0.5 is present. Only Raman scattering is considered in the model.
Note: the x axis is 0.8 to 1.0 instead of 0.0 to 1.0.

In Fig. 7, data from shallow stations are presented together with the model results. One might think that coastal water is very rich in both chlorophyll and DOM and that the inelastic scattered light must be a big portion of the light field. This is incorrect. Not only is the inelastic component in the downwelling light field negligible, but this is also true in the upwelling light field. Even for upwelling, in the total light field, the inelastic light portion is less than 4% at surface, which is less than the instrument error (5%). As a contrast, this value is generally greater than 10% in clear waters (Fig. 6). This difference is due to the bottom effect. The bottom reflected light occupies a big portion in the total upwelling light field. Thus, the inelastic portion is very small. Simulation results show this is also true even when the water is rich in DOM and chlorophyll, or the bottom reflectance is low. So, for shallow waters, the inelastic light is negligible in either downwelling or upwelling light fields.

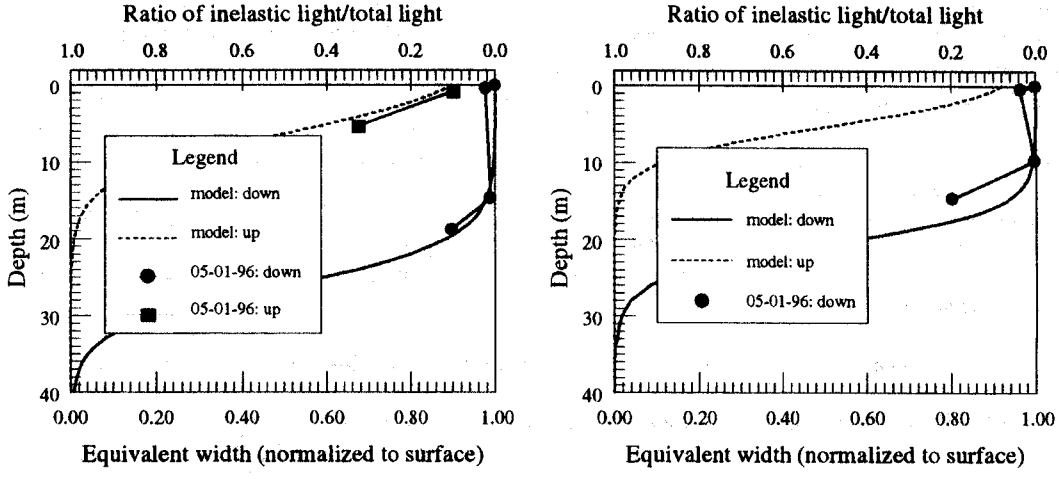

Figure 8. Experimental data from clear ocean water and Monte-Carlo simulation results for the Fraunhofer line at 656nm (left) and for the oxygen absorption line at 689nm (right). Only Raman scattering is considered in the model.

From the results shown above, it can be seen that the technique for using the Fraunhofer lines as inelastic scattering indicators is very powerful in studying *in situ* inelastic light scattering processes in natural waters. Using the same idea, smaller oxygen absorption lines around 689nm (Fig. 3) are utilized to study the *in situ* chlorophyll fluorescence at 685nm. Figure 8 shows that even in clear water where at 656nm the inelastic light is mainly from Raman scattering, the signal from chlorophyll fluorescence is detectable at 689nm. Note that these data were taken at the same station. This will enable us to measure the natural fluorescence in the future.

4. CONCLUSION

The prototype Fraunhofer instrument system[10] has been rebuilt and improved. The correct Raman scattering coefficient at any λ is determined by using the clear water data and the Monte-Carlo simulation and can be used as a basis when other inelastic components, e.g., fluorescence, are considered. Small absorption lines at 689nm are used to detect the chlorophyll fluorescence at 689nm. This has proved to be a promising technique to measure the natural fluorescence.

5. ACKNOWLEDGMENTS

The work is supported by the Ocean Optics program of the Office of Naval Research. The authors want to express their gratitude to Mr. Albert Chapin, who helped a lot in the instrument rebuild, and to Dr. Howard Gordon, Dr. Yuntao Ge and Mr. Marco Monte for very helpful discussions in the simulations.

6. REFERENCES

1. B.R. Marshall and R.C. Smith, "Raman Scattering and In-Water Ocean Optical Properties," Appl. Opt. **29**(1), 71-84 (1990).
2. R.B. Slusher and V.E. Derr, "Temperature Dependence and Cross Sections of some Stokes and Anti-Stokes Raman Lines in Ice Ih," Appl. Opt. **14**(9), 2116-2120 (1975).
3. S. Sugihara, M. Kishino and N. Okami, "Contribution of Raman Scattering to Upward Irradiance in the Sea," Jour. Oceanogr. Soc. Japan **40**, 397-404 (1984).
4. R.H. Stavn and A.D. Weidemann, "Optical Modeling of Clear Ocean Light Fields: Raman Scattering Effects," App. Opt. **27**(19), 4001-4011 (1988).
5. R.H. Stavn, "Raman Scattering Effects at the Shorter Visible Wavelengths in Clear Ocean Water," SPIE Ocean Optics **X 1302**, 94-100 (1990).
6. H.R. Gordon, "The Diffuse Reflectance of the Ocean: The Theory of Its Augmentation by Chlorophyll a Fluorescence at 685nm," Appl. Opt. **18**, 1161-1166 (1979).
7. F.E. Hoge and R.N.Swift, "Airborne Simultaneous Spectroscopic Detection of Laser-Induced Water Raman Backscatter and Fluorescence from Chlorophyll a and Other Naturally Occurring Pigments," Appl. Opt. **20**, 3197-3205 (1981).
8. G.W. Kattawar and X. Xu, "Filling In of Fraunhofer Lines in the Ocean by Raman Scattering," Appl. Opt. **31**(30), 6491-6500 (1992).
9. Y. Ge, H.R. Gordon and K.J. Voss, "Simulation of Inelastic-Scattering Contributions to the Irradiance Field in the Ocean: Variation in Fraunhofer Line Depths," Appl. Opt. **32**(21), 4028-4036 (1993).
10. Y. Ge, K.J. Voss and H.R. Gordon, "In Situ Measurement of Inelastic Ligh Scattering In Monterey Bay Using Solar Fraunhofer Lines," Journal of Geophysical Research, **100**(C7), 13227-13236 (1995).